Far field diffraction of an optical vortex beam by a fork-shaped grating

Lyubomir Stoyanov[1], Suzana Topuzoski[2], Ivan Stefanov[1], Ljiljana Janicijevic[2] and Alexander Dreischuh[1,2,*]

[1] *Department of Quantum Electronics, Faculty of Physics, Sofia University "St. Kliment Ohridski", Sofia-1164, Bulgaria*

[2] *Faculty of Natural Sciences and Mathematics, Institute of Physics, University Ss. Cyril and Methodius, Skopje-1000, Republic of Macedonia*

compiled: January 11, 2015

In this work we report experimental data confirming the predicted transformation of the topological charge (TC) of an input optical vortex (OV) beam, generated by means of fork-shaped binary computer-generated hologram (CGH), after a second fork-shaped binary CGH. The final TC of the vortex is confirmed to be equal to the TC of the incident beam plus the diffraction order (with its sign) times the TC encoded in the binary grating. The radii of the transformed OVs in the far field also are found to agree fairly well with these predicted by the analytical theory.

OCIS codes: (050.1960) Diffraction theory; (050.1970) Diffractive optics; (260.6042) Singular optics; (050.4865) Optical vortices.

http://dx.doi.org/10.1364/XX.99.099999

1. Introduction

Recent years have seen an increased interest and research about the optical fields possessing screw phase singularities carried by optical vortex beams. The transverse cross-sections of the optical vortices (OVs) are associated with isolated point singularities with helical phase wavefront around them. The central singular point of the helix possesses undefined phase and therefore the intensity must vanish, leading to a characteristic toroidal intensity profile (vortex ring). The study of the phase singularities is important from the viewpoint of both fundamental as well as applied physics. Light beams possessing phase singularities are used in the experiments for particle trapping and manipulation [1], atom trapping and guiding [2], as information carriers [3] for multiplexing in free-space communications [4], for interferometry [5], and for realizing of electron vortex beams [6], just to mention a few.

Only 20 years ago, the Laguerre-Gaussian (LG) laser modes having an azimuthal mode number different from zero (eigen modes of a laser cavity described in cylindrical coordinates) and other vortex beams having helical wavefront structure with phase dependence $\exp(il\varphi)$ (where l is an integer and φ is the azimuthal coordinate) were recognized to have orbital angular momentum (OAM) $l\hbar$ per photon in their propagation direction [7]. The number l showing the total phase change $2\pi l$ over the azimuthal coordinate φ is referred as the topological charge of the OV beam. It was shown that this OAM can be transferred to a captured microparticle causing its rotation in a direction determined by the sign of the topological charge (TC) [8].

The intensive research in the field of singular optics has shown that optical vortex beams can be generated from incident chargeless optical beams by means of diffractive optical elements (DOEs) with embedded phase dislocations, such as spiral phase plate (SPP) [9], helical axicon [10], computer-generated holograms [11], spiral zone plates [12] as well as fork-shaped gratings [13–15]. Some of them, when build in dispersionless optical systems, provide a useful means to create phase singularities in the beams of ultrafast femtosecond lasers with broad bandwidth [16–18]. OV creation succeeded even in near-single-cycle regime of ultrashort laser pulse generation [19] by using thermally tuning reflective spiral micro-electro-mechanical elements [20]. The transformation of the incident vortex beam through some types of DOEs with encoded phase singularities was studied in details in [21, 22]. In [21] the authors have shown theoretically that in the process of diffraction of LG beam with zeroth radial mode number and arbitrary azimuthal mode number l, by a fork-shaped grating with integer forked dislocations p, in the positive and negative m-th diffraction order, the diffracted beam carries topological charge s which is determined as an algebraic

* Corresponding author: ald@phys.uni-sofia.bg

sum $s = l + mp$ or $s = l - mp$, respectively. In the paper of Mair and co-authors [23] a fork-shaped grating is used as a filter for estimating the TC of optical vortices.A photon with angular momentum $p\hbar$ before the fork-shaped grating which possesses phase singularity of order p, can be detected by a mono-mode fiber detector placed in the negative first diffraction order. In the same setup a photon with zero angular momentum can be detected by diffracting the beam far away from the forked section of the grating where the grating isi nearly rectilinear. In this experiment [23] the authors confirmed the conservation of the OAM of (entangled) photons in the process of spontaneous parametric down-conversion. Soskin and co-authors [24] have studied theoretically and experimentally the behavior of vortices in a beam composed from singular and background Gaussian waves, in order to check the principle of TC conservation. The topological charge in nonlinear optics has been studied by Soskin et al. [25] who suggested its conservation in a stimulated down-conversion process. The experiment of Maleev et al. [26] has not shown, however, any evidence of topological charge conservation. It was recently shown that the TC conversion in cascaded four-wave frequency mixing process obeys the transformation law analogous to the one for the frequency [27]. The conservation of the TC was demonstrated for the surface plasmons: when the LG beam having azimuthal mode number l is transferred through plasmonic vortex lens with TC equal to m, then surface plasmon vortices with orbital angular momentum are generated, and inherit the optical angular momentum of light beams and plasmonic vortex lens, since their topological charge n was equal to $n = l + m$ [28].

The aim of this work is to confirm experimentally the predicted [21, 29] transformation of the topological charge of the incident vortex beam during the transfer through a fork-shaped grating with embedded topological defects of integer number. For this purpose we generate OVs with TCs equal to 2, 3 and 4 by fork-shaped gratings and let them, subsequently, diffract to the far field by another singled- and twofold-charged fork-shaped gratings. The reversed case is also studied. The theoretical results [21, 29] for the algebraic transformation of the TCs of the OVs were checked by making interferograms of the diffracted components and a plane wave, while the vortex ring radii of the transformed beams were compared by using their radial intensity profiles.

2. Theoretical background

In the experiment described and illustrated by the setup in Fig. 1, the vortex beam passing normally through the bottom of the fork-shaped area of the grating 2 (CGH2), is previously generated by letting a chargeless Gaussian laser beam to pass normally through the fork-shaped grating 1 (CGH1). The Gaussian beam axis is passing through the centre of the forked dislocation of the CGH1, where the pole of the cylindrical system with coordinates r', φ' and z' is situated. The gratings possess TCs p_1 and p_2 , respectively, which are encoded in the fork-shaped singularities. Recalling the theoretical results in [29], in the process of Fresnel diffraction the grating 1 (situated in a plane $z' = 0$ splits the incident Gaussian beam $U'(r', \varphi', z' = 0) = \exp(-r'^2/w_0'^2)$ (where w_0' is its waist radius) into a fan of beams. The direct zeroth-diffraction-order beam is a chargeless Gaussian beam. The higher positive and negative m'-th diffraction-order beams appear as optical vortex beams carrying phase singularities with TCs $m'p_1$ and $-m'p_1$, respectively. This can be seen from expression (17) in the same article. In our experiment we will use expression (17) adapted to the so-called far-field approximation (where the distance between the two gratings is such that $1/R(z') \to 0$, $1/z' \to 0$, $Q^{-1}(z') = (1/2)[(R^{-1}(z') - z'^{-1}) - 2i/(kw^2(z'))] \to -i/(kw^2(z'))$, and $\exp[i \arctan(2z'/kw_0'^2)] \to 1$). Also, we are interested in the paraxial region of the OV beam distribution $0 \le r_{\pm m'} \le w(z')$, (instead of the coordinates $\rho_{\pm m}$ and $\vartheta_{\pm m}$ in Eq. (17) from [29] we use polar coordinates $r_{\pm m'}$ and $\varphi_{\pm m'}$, and denote with $w(z')$ the vortex beam amplitude profile radius at position z'). Therefore, we will neglect all $n \neq 0$ members in the sum by which the Kummer function is represented, i.e. for the far field $M(|m'p_1|/2, |m'p_1| + 1, r^2_{\pm m'}/w^2(z')) \approx 1$. In this approximation the m'-th diffraction order beam, emerging from the CGH1, is described by the expression

$$U_{\pm m'}(r_{\pm m'}, \varphi_{\pm m'}, z') = C_{m'p_1} \left[\frac{r_{\pm m'}\sqrt{2}}{w(z')}\right]^{|m'p_1|} \times \exp\left(-\frac{r^2_{\pm m'}}{w^2(z')}\right) \exp[-i(kz' \mp m'p_1\varphi_{\pm m'})]. \quad (1)$$

Here $C_{m'p_1}$ is the complex amplitude given by

$$C_{m'p_1} = \frac{w_0'}{w(z')} t_{\pm m'} \frac{\Gamma(|m'p_1|/2 + 1)}{\Gamma(m'p_1 + 1)\sqrt{2^{|m'p_1|}}} \exp(im'p_1\pi/2) \quad (2)$$

with $t_{\pm m'}$ being the transmission coefficients of the first grating [29]. Expression (1) is recognized as zero radial mode LG laser beam with azimuthal mode number $\pm m'p_1$ equal to its phase singularity order. The same approximation for the higher diffraction orders of the beams generated by fork-shaped grating is used by the authors in [14, 30–32].

In our experiment z' is the distance between the two gratings. The incident beam on the second grating carrying TC $p_2 = p$ is selected by the first diaphragm (Fig. 1). It is a vortex beam of type (1) with TC $l = m'p_1$ having entrance radius $w(z') = w_0$ of the transverse amplitude profile. Instead of the coordinates $(r_{\pm m'}, \varphi_{\pm m'}, z')$ now, for simplicity, we will use (r, φ, z), and take l to be a positive integer. Thus, the incident beam on the second fork-shaped grating is approximated as $LG_0^{(l)}$ mode

$$U_0^{(l)}(r, \varphi, z = 0) = A_{l,0}(r\sqrt{2}/w_0)^l \exp(-r^2/w_0^2) \exp(il\varphi), \quad (3)$$

where $A_{l,0}$ is an amplitude coefficient.

Further, we threat the Fraunhofer (far-field) diffraction of this singular field by the second fork-shaped grating with an encoded topological charge p, having transmission function in polar coordinates as follows

$$T(r,\varphi) = \sum_{m=-\infty}^{\infty} t_m \exp\{-im[(2\pi/D)r\cos(\varphi) - p\varphi]\}. \tag{4}$$

The transmission coefficients of this binary amplitude grating are: $t_0 = 1/2$, $t_{\pm m=\pm(2n'-1)} = \mp i/[\pi(2n'-1)]$, $t_{\pm m=\pm 2n'} = 0$ $(n' = 1, 2, 3...)$. The constant D is the grating period far from its pole. The theoretical results for the problem of Fraunhofer diffraction of $LG_0^{(l)}$ beam incident with its waist on a fork-shaped grating are presented in [21]. We will recall here to the main results: the diffracted wave field amplitude U in the focal plane with coordinates ρ and θ of a convergent lens with focal length f is calculated as a sum of a zeroth-diffraction-order beam (U_0) and higher, positive (U_{+m}) and negative (U_{-m}) diffraction-order beams, deviated from the incident beam axis z

$$U(\rho,\theta,f) = U_0(\rho,\theta,f) + \sum_{m=1}^{\infty} U_{+m}(\rho_{+m},\theta_{+m},f) + \sum_{m=1}^{\infty} U_{-m}(\rho_{-m},\theta_{-m},f). \tag{5}$$

The pairs of variables (ρ_{+m},θ_{+m}) and (ρ_{-m},θ_{-m}) in the focal plane play the role of plane polar coordinates, related to the centres of the higher-diffraction-order beams, $C_{+m}(m\lambda f/D, 0)$ and $C_{-m}(m\lambda f/D, \pi)$, respectively [29].

In the focal plane the zeroth-diffraction-order beam is found as a LG beam with a phase singularity of topological charge l along its propagation axis ($\rho = 0$), where it has a vanishing amplitude

$$U_0(\rho,\theta,f) = A_{l,0} i(w_0/w_f) t_0 \exp[il(\theta+\pi/2)] \times (\sqrt{2}\rho/w_f)^l \exp(-\rho^2/w_f^2). \tag{6}$$

In the last equation the notation $w_f = \lambda f/(\pi w_0)$ for the $LG_0^{(l)}$ beam waist radius for a focusing lens of a focal length f is used (λ is the incident beam wavelength). The beams in the higher positive and negative diffraction orders are deviated from the z axis (the transverse Cartesian coordinate system axis, which is perpendicular to the grating stripes). They have wave amplitudes described by a product of a Gauss-doughnut function $(\rho_{\pm m}/w_f)^{|s_{\pm m}|}\exp(-\rho_{\pm m}^2/w_f^2)$ of order $|s_{\pm m}|$ and a confluent hypergeometric (Kummer) function M

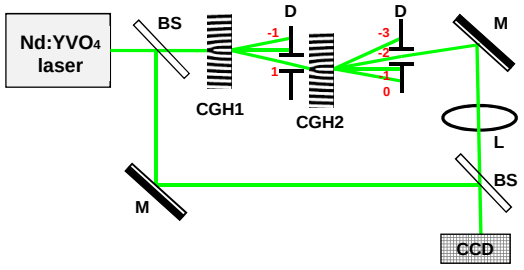

Fig. 1. **Experimental setup**: $Nd:YVO_4$ laser - continuous-wave frequency-doubled laser emitting at a wavelength of $532nm$. BS - beam splitters. CGH1, CGH2 - binary computer-generated holograms. D - iris diaphragms. L - focusing lens ($f = 100cm$). M - flat mirrors. CCD - charge-coupled device camera located at the beam waist.

$$U_{\pm m}(\rho_{\pm m},\theta_{\pm m},f) = A_{l,0} i(w_0/w_f) t_{\pm m} 2^{l/2} \times \exp[is_{\pm m}(\theta_{\pm m} \pm \pi/2)] \left(\frac{\rho_{\pm m}}{w_f}\right)^{|s_{\pm m}|} \times \exp\left(-\frac{\rho_{\pm m}^2}{w_f^2}\right) \frac{\Gamma((|s_{\pm m}|+l)/2+1)}{\Gamma(|s_{\pm m}|+1)} \times M\left(\frac{|s_{\pm m}|-l}{2}, |s_{\pm m}|+1; \frac{\rho_{\pm m}^2}{w_f^2}\right), \tag{7}$$

where the following signs are introduced

$$s_{+m} = l + mp; s_{-m} = l - mp; (m = 1, 2, ...); s_{m=0} = l. \tag{8}$$

From Eq. 7 it can be concluded that, in the $\pm m$-th diffraction order, a phase singularity of $|s_{\pm m}|$-th order occurs (except for the case when $l - mp = 0$ is satisfied). The topological charge is equal to $l + mp$ and $l - mp$, respectively, for the positive and negative m-th-diffraction-order beams. The transverse intensity profile of the singular beam is a vortex ring with a dark core, whose radius in the m-th diffraction order, characterized by TC s, (see Eq. (16) in [21]) is calculated approximately as

$$\rho_{max,s} = w_f \sqrt{\frac{(|l \pm mp| + 1)|l \pm mp|}{|l \pm mp| + l + 2}} = w_f \sqrt{\frac{(|s_{\pm m}| + 1)|s_{\pm m}|}{|s_{\pm m}| + l + 2}}. \tag{9}$$

Further we will present our experimental scheme and the obtained results for the transformation of the TCs of the OVs as well as data for the vortex ring radii, and will compare them to the above theoretical results.

3. Experimental setup and results

The experimental setup we used is shown in Fig. 1. The beam of a continuous-wave frequency-doubled $Nd:YVO_4$ laser at a wavelength of $532nm$ is first split by a

beam splitter (BS) and, later, the object and the reference beams are recombined by a second BS to interfere at the CCD camera chip. The CCD camera is carefully located at the beam waist of the focusing lens L (focal length $f = 100cm$). In the object arm of the interferometer the beam illuminates the first binary computer-generated hologram (CGH1). Both used holograms are fork-shaped amplitude diffraction gratings produced photolithographically with a grating period of $30\mu m$. In these holograms we encoded point (fork-like) phase singularities with spiral phase profiles (OVs) with TCs ranging from 1 to 4.The laser beam diffracts from CGH1 and the desired diffraction order beam with the desired TC is transmitted by the first iris diaphragm D. Further we will call it an incident beam (approximated by Eq. 3). This incident beam illuminates the second computer-generated hologram CGH2 and the desired diffraction order beam is selected by the second iris diaphragm D. In this way the object beam is formed. Power density distributions of the resulting optical vortex beams and the respective interference patterns are recorded by the same CCD camera by blocking/unblocking the reference laser beam but keeping the camera position unchanged.Theh results presented in this paper are selected out of a much wider set of measurements with different combinations of the OV TCs l and p.

The first main theoretical result given by Eq. 8 states that the final TC s of the vortex should be equal to the TC l of the incident beam plus the diffraction order m (with its sign) times the TC p encoded in the binary grating (CGH2, see Fig. 1):

$$s = l + mp. \tag{10}$$

In Fig. 2 we show in a simple way what should be the TC s of the output OV after fulfillment of this transformation rule in the simple case of $l = 2$ and $p = 1$, in different diffraction orders. The relative size of the black circles is chosen to qualitatively reflect the fact that the higher the (absolute value of the) topological charge, the broader the dark OV core and the higher the radius of the bright vortex ring. In one of the cases one should expect that the TC of the incident OV beam will be "erased" and the TC of the output beam should be zero. Therefore, there will be no reason to observe a dark beam nested on the bright background. In Fig. 2 this case is present in the (-2)-nd diffraction order. Since in different diffraction orders OVs with equal, as an absolute value, but opposite in sign TCs are expected, the TC sign change is identified by the reversal of the fork-like splitting of one of the interference stripes in the recorded interference patterns.

3.A. Case A: $l = 2$ and $p = 1$

In Fig. 3 we present experimental data for the case when the incident beam carries a twofold-charged OV ($l = 2$) and a singly-charged OV is encoded in the binary grating CGH2 (see Fig. 1; i.e. $p = 1$). In the first column of

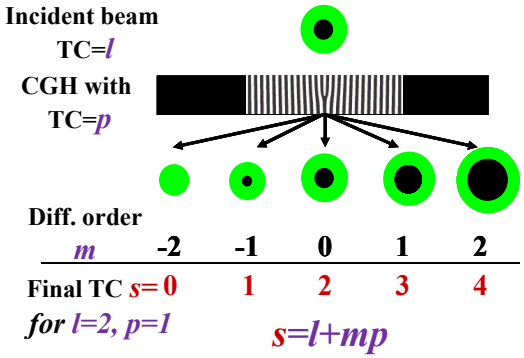

Fig. 2. Sketch of the TC transformation rule (Eqs. 8) in the case of $l = 2$ and $p = 1$.

this figure, as well as in Figs. 5,7, and 9, we show power density distributions of the diffracted beams in the focal plane of the focusing lens. Especially intriguing is the result for the diffraction in the -2-nd order ($m = -2$). According to the TC transformation rule the resulting topological charge is zero ($s = 2+(-2)1 = 0$) and we observed a beam with a well formed single peak. This peak was observed in the focal plane of the lens only. Shifting the CCD camera around this position we observed flat-topped and even (at larger offsets) only partially filled doughnut-like beams. The respective interferogram consists of parallel interference lines confirming that the TC of the input beam is "erased" (i.e. set to zero). For the negative diffraction orders $m = -3$ and -4 the TC of the resultant beam is negative ($s = -1$ and -2, respectively), and the fork-like splitting of one interference line in 2 and 3 lines is directed downwards. For the ± 1-st and for the 0-th diffracted order beams, as predicted, the resultant TCs s are positive. This is clearly seen in the respective interferograms, in which the fork-like splitting of the interference line is upwards. The experimentally obtained TCs confirm that the predicted TC transformation rule holds in this case. In Fig. 4 we show the normalized radial cross-sections of all OV beams and of the chargeless beam, experimentally generated in this case ($l = 2$ and $p = 1$) in different diffraction orders and notation of their final TCs. For better visibility in all such comparisons in this manuscript we normalized the OV ring peaks to unity avoiding the visual effects of the very different (decreasing) diffraction efficiency of CGH2 with increasing the diffraction order m. This is valid also for the Figures 6, 8 and 10. Qualitatively, the higher the absolute value of the OV TC, the broader the vortex ring. The second main theoretical result from [21] given here by Eq. 9 gives much more - an analytical estimate of the vortex ring radii $\rho_{max,s}$ in different diffraction orders m, depending on the input TC l and on the TC p encoded in the second CGH. By using that equation we calculated the vortex ring radii $\rho_{max,s}$ (for different l, p and m values) of the exit beam carrying TC s, normalized to the vortex ring radius ρ_1 of the singly-charged exit beam (for cases A, B and C). On the

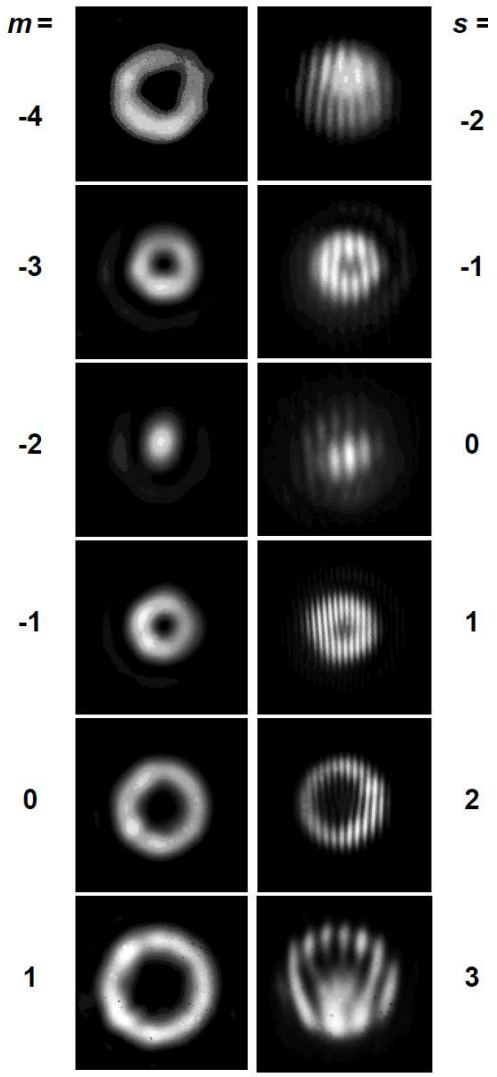

Fig. 3. **Case A:** $l = 2$ **and** $p = 1$**.** Power density distributions of the OV beams diffracted in different orders m of CGH2 with an encoded singly-charged OV (left column) and respective interferograms for identifying the resultant OV TC s (right column).

other hand side we estimated these normalized vortex radii ρ_s/ρ_1 from the experimentally obtained intensity distributions given in Figures 4, 6 and 8 (respectively for the cases A, B and C). Further we present the comparison between the theoretical and experimental values ofo the relations ρ_s/ρ_1 for cases A, B and C in Table 1. In Table 2, however, by necessity, we present such a comparison for the vortex ring radii normalized to the double-charged vortex beam, ρ_s/ρ_2 (case D).

3.B. Case B: $l = 3$ and $p = 1$

In Fig. 5, following the same style of presentation, we show experimental data for the case when the incident beam carries a threefold-charged OV ($l = 3$) and, as in the previous case, a singly-charged OV ($p = 1$) is encoded in the binary grating CGH2. All final topological

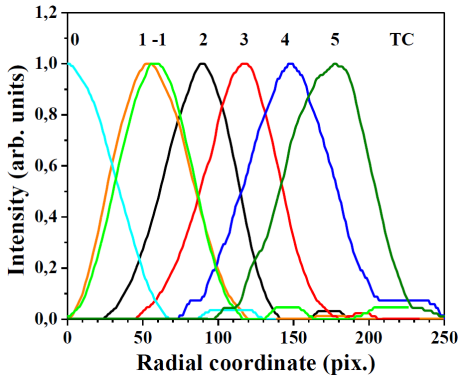

Fig. 4. Normalized radial cross-sections of the OV beams experimentally generated in **Case A** ($l = 2$ and $p = 1$) in different diffraction orders and their TCs.

charges retrieved from the experiment confirm the theoretical prediction in both modulus and sign of the TC (see right column in Fig. 5, the number of split interference lines and the direction of splitting). As in **Case A**, this time in the -3-rd diffraction order, the TC=3 of the incident OV beam is erased and a well formed single peak is seen in the beam waist. Note that for $s = 3$ and 4 the multiply-charged OVs split into singly-charged ones but they still remain with highly overlapping cores. For $s = 4$ the vortex ring shows a weak azimuthal modulation which is a result of the binary nature of the holograms we used. As in the previous case, the respective radial cross-sections of the recorded vortex rings are shown in Fig. 6. Ones again, in an agreement with the physical intuition, the higher the absolute value of the OV TC, the broader the vortex ring.

3.C. Case C: $l = 4$ and $p = 1$

In Fig. 7 experimental data for the case of an incident beam carrying a fourfold-charged OV ($l = 4$) are shown. As in the previous two cases, a singly-charged OV ($p = 1$) is encoded in the binary grating CGH2. In the -4-th diffraction order one can see the "erasure" of TC=4 and formation of a single bright peak in the former large vortex core. In the middle of the corresponding interference pattern the interference lines are parallel, which is an indication for a flat phase profile. Across a dark ring surrounding the central dominating peak the outer parts of the interference stripes are shifted with respect to the central part, which is an indication for the existence of a surrounding ring dark wave. Such structure can be seen also in **Case B** for $m = -3$ and $s = 0$. Generally, the interference patterns observed in this case (Fig. 7, right column) ones again confirm the theoretically predicted TC transformation rule. The OV ring radii obviously increase with increasing the final topological charge s, which is also clearly seen in Fig. 8. In the vortex ring of the charge 5 OV one can see an azimuthal modulation which is a result of the binary nature of the holograms we used. The evaluated

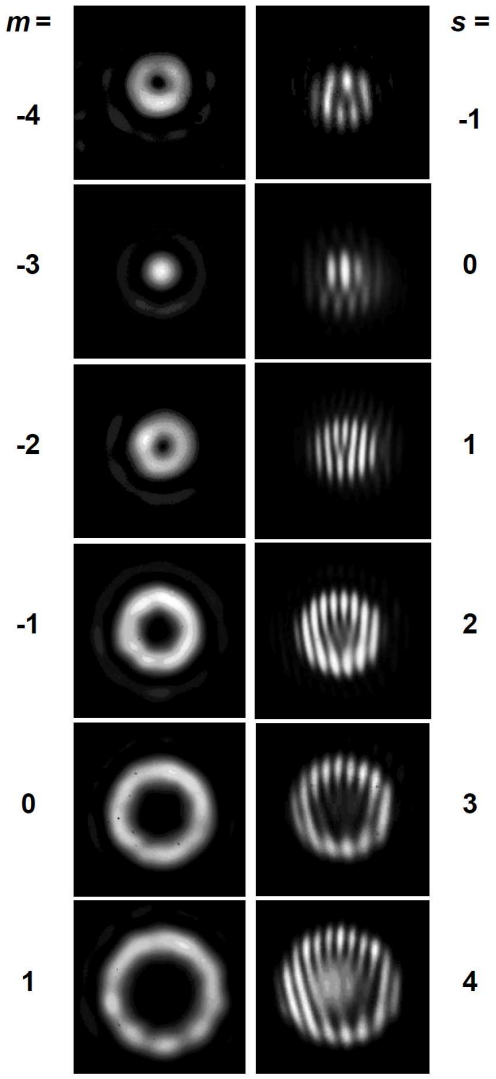

Fig. 5. **Case B:** $l = 3$ **and** $p = 1$**.** Power density distributions of the OV beams diffracted in different orders m of CGH2 with an encoded singly-charged OV (left column) and respective interferograms for identifying the resultant OV TC s (right column).

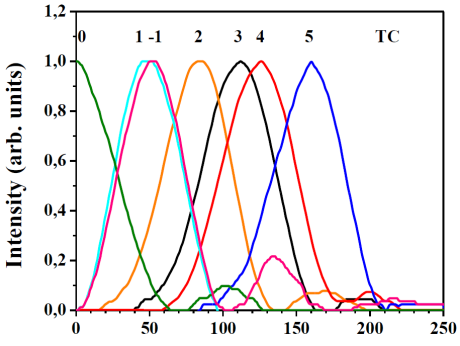

Fig. 6. Normalized radial cross-sections of the OV beams experimentally generated in **Case B** ($l = 3$ and $p = 1$) in different diffraction orders and their TCs.

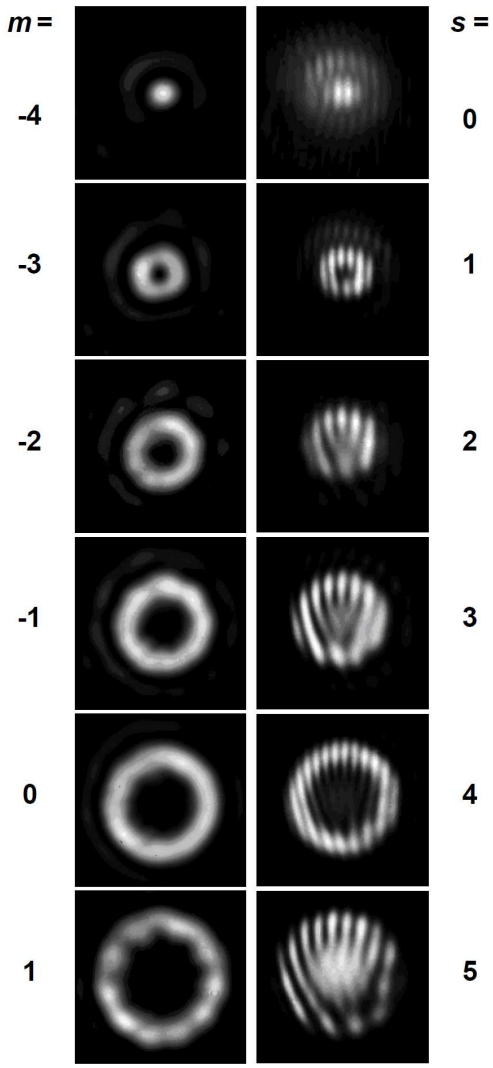

Fig. 7. **Case C:** $l = 4$ **and** $p = 1$**.** Power density distributions of the OV beams diffracted in different orders m of CGH2 with an encoded singly-charged OV (left column) and respective interferograms for identifying the resultant OV TC s (right column).

radius of this slightly modulated OV ring, however, perfectly matches the theoretical prediction (see **Case C**, $\rho_5/\rho_1 = 3.11$ in Table 1).

In Table 1 we present a comparison between the theoretically predicted (th.) and experimentally estimated (exp.) vortex ring radii ρ_s normalized to the ring radius ρ_1 of the singly-charged OV ring for **Cases A, B**, and **C**. In most cases the discrepancy is well below 10% and one can say that the experimental data fairly well confirm the theoretical prediction given by Eq. 9.

3.D. Case D: $l = 4$ to $p = 2$

This is the last case (see Fig. 9), which we would like to present out of the much wider set of measurements with different combinations of TCs l and p. Here the diffraction takes place from a CGH2 in which a twofold-charged

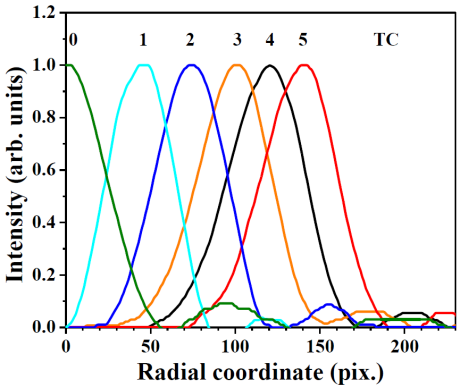

Fig. 8. Normalized radial cross-sections of the OV beams experimentally generated in **Case C** ($l = 4$ and $p = 1$) in different diffraction orders and their final TCs.

Table 1. Comparison between the theoretically predicted and experimentally estimated vortex ring radii ρ_s normalized to the ring radius ρ_1 of the singly-charged OV ring for **Cases A, B**, and **C**. (n.a. – this case is not available experimentally.)

Case		(ρ_{-1}/ρ_1)	(ρ_2/ρ_1)	(ρ_3/ρ_1)	(ρ_4/ρ_1)	(ρ_5/ρ_1)
A	th.	1	1.58	2.07	2.51	2.90
	exp.	1.06	1.64	2.12	2.63	3.18
B	th.	1	1.60	2.10	2.57	2.98
	exp.	1.09	1.68	2.20	2.52	3.16
C	th.	n.a.	1.64	2.19	2.66	3.11
	exp.	n.a.	1.64	2.22	2.66	3.11

OV is encoded. Hence, by changing from one diffraction order to the neighboring one, the final OV topological charge changes by 2. We selected to present here this case because for $p = 3$ and 4 the TCs of the diffracted waves increase by 3 and 4, respectively. Unfortunately, for topological charges higher than 6, we observed more or less pronounced OV ring azimuthal modulation due to the binary nature of the gratings used. Once again, all general features of the recorded power density and interference distributions of the output OVs are in agreement with the preceding observations:

i) The proposed OV TC transformation rule holds precisely.;

ii) OV TC can be erased which leads to a well formed single bright peak at the former position of the OV dark core.;

iii) The bright OV ring radii increase with increasing the modulus of the OV TC (see Fig. 10).;

iv) The normalized OV ring radii retrieved from the experiment agree qualitatively with the theoretical prediction (see Table 2).

4. Conclusion

The presented experimental data confirm the predicted transformation of the topological charge of an incident optical vortex beam after a second fork-shaped binary

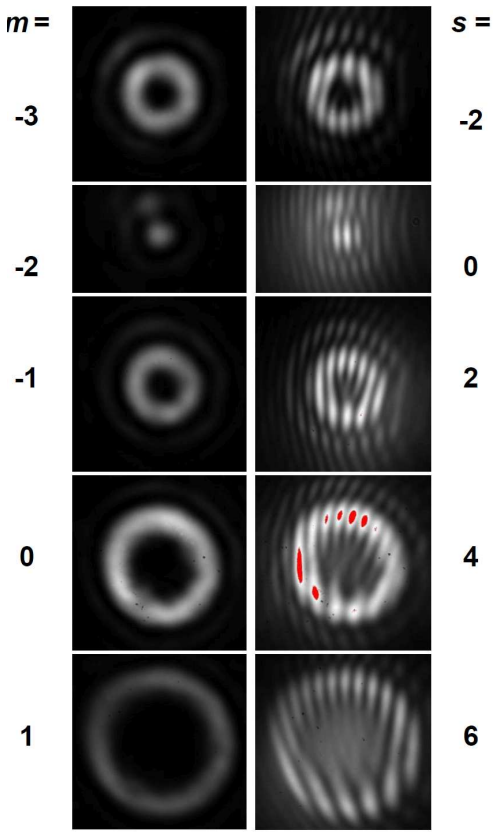

Fig. 9. **Case D:** $l = 4$ **and** $p = 2$**.** Power density distributions of the OV beams diffracted in different orders m of CGH2 with an encoded twofold-charged OV (left column) and respective interferograms for identifying the resultant OV TC s (right column).

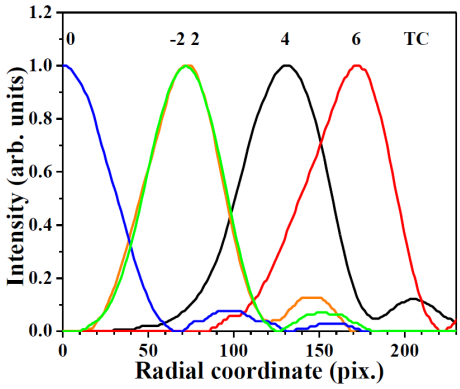

Fig. 10. Normalized radial cross-sections of the OV beams experimentally generated in **Case D** ($l = 4$ and $p = 2$) in different diffraction orders and their TCs.

computer-generated hologram: The final TC of the vortex is equal to the TC of the incident beam plus the diffraction order (with its sign) times the TC encoded in the binary grating. As a consequence from this transformation rule, OV TC can be erased in one case when the resultant TC equals to zero. As a result, in the fo-

Table 2. Comparison between the theoretically predicted and experimentally estimated vortex ring radii ρ_s normalized to the ring radius ρ_2 of the twofold-charged OV ring for **Case D**.

Case D	(ρ_{-2}/ρ_2)	(ρ_4/ρ_2)	(ρ_6/ρ_2)
th.	1	1.63	2.15
exp.	0.99	1.79	2.35

cal plane of a lens (and in the far field) a well formed single bright peak is formed at the former position of the OV dark core. The theoretical results [21, 29] for the algebraic transformation of the TCs of the OVs and for the vortex ring radii of the transformed beams vs. final TC are found in a perfect agreement with the experimental data. By using such experimental setup an one-dimensional array of OVs (on their own background beams) with different values and signs of their TCs can be produced, including a beam which does not possess a phase singularity. Each of the diffraction-order beams in that array can be focused into a separate optical trap. If the OV TC is non-zero it will have a dark vortex core and carry orbital angular momentum with a specific value (suitable for trapping low-index micrometer-sized particles or atoms), or can be with a chargeless bright core (if the TC is zero; suitable for trapping particles with higher refractive index than that of surrounding medium) [33]. By using different diffraction order beams one can arrange two near-by optical vortices with opposite wavefront helicities to exert torques with opposite directions that together can be used to create a microfluidic pump [34], just to mention two ideas for application of such OVs.

5. Acknowledgments

We gratefully acknowledge financial support of the National Science Fund (Bulgaria) within the framework of project FNI-T02/126 and project BG051 PO001-3.3.06-0057.

References

[1] D. G. Grier, "A revolution in optical manipulation," Nature **424**, 810–6 (2003).
[2] N. Friedman, A. Kaplan, and N. Davidson, "Dark optical traps for cold atoms," Adv. in Atomic, Molecular and Optical Physics (Elsevier Science, 2002), 101–106 (2002).
[3] G. Molina-Terriza, J. P. Torres, and L. Torner, "Twisted photons," Nature Physics **3**, 305–310 (2007).
[4] J. Wang, J.-Yu. Yang, I. M. Fazal, N. Ahmed, Y. Yan, H. Huang, Y. Ren, Y. Yue, S. Dolinar, M. Tur, and A. E. Willner, "Terabit free-space data transmission employing orbital angular momentum multiplexing," Nature Photonics **6**, 488–496 (2012).
[5] S. Furhapter, A. Jesacher, S. Benet, and M. R. Marte, "Spiral interferometry," Opt. Lett. **30**, 1953–1955 (2005).
[6] R. Van Boxem, J. Verbeeck, and B. Partoens, "Spin effects in electron vortex states," Europhys. Lett. **102**, 40010 (2013).
[7] L. Allen, M. W. Beijersbergen, R. J. C. Spreeuw, and J. P. Woerdman, "Orbital angular momentum of light and the transformation of Laguerre-Gaussian laser modes," Phys. Rev. A **45**, 8185–8189 (1992).
[8] H. He, M. E. J. Friese, N. R. Heckenberg, and H. Rubinsztein-Dunlop, "Direct observation of transfer of angular momentum to absorptive particles from a laser beam with a phase singularity," Phys. Rev. Lett. **75**, 826–829 (1995).
[9] S. N. Khonina, V. V. Kotlyar, M. V. Shinkaryev, V. A. Soifer, and G. V. Uspleniev, "The phase rotor filter," J. Modern Optics **39**, 1147–1154 (1992).
[10] S. N. Khonina, V. V. Kotlyar, V. A. Soifer, M. V. Shinkaryev, and G. V. Uspleniev, "Trochoson," Optics Commun. **91**, 158–162 (1992).
[11] A. Vasara, J. Turunen, and A. T. Friberg, "Realization of general nondiffracting beams with computer-generated holograms," J. Opt. Soc. Am. A **6**, 1748–1754 (1989).
[12] N. R. Heckenberg, R. McDuff, C. P. Smith, and A. G. White, "Generation of optical phase singularities by computer generated holograms," Opt. Lett. **17**, 221–223 (1992).
[13] V. Yu. Bazhenov, M. V. Vasnetsov, and M. S. Soskin, "Laser beams with screw dislocations in their wavefronts," Pisma Zh. Eksp. Teor. Fiz. **52**, 1037–1039 (1990).
[14] N. R. Heckenberg, R. McDuff, C. P. Smith, H. Rubinsztein-Dunlop, and M. J. Wegener, "Laser beams with phase singularities," Opt. Quant. Electron. **24**, S951–S962 (1992).
[15] B. Terhalle, A. Langner, B. Päivänranta, V. A. Guzenko, C. David, and Y. Ekinci "Generation of extreme ultraviolet vortex beams using computer-generated holograms," Opt. Lett. **36**, 4143–4145 (2011).
[16] K. Bezuchanov, A. Dreischuh, G. G. Paulus, M. G. Schätzel, and H. Walther, "Vortices in femtosecond laser fields," Opt. Lett. **29**, 1942–1944 (2004).
[17] I. G. Mariyenko, J. Strohaber, and C. J. G. J. Uiterwaal, "Creation of optical vortices in femtosecond pulses," Opt. Express **13**, 7599–7608 (2005).
[18] K. Bezuchanov, A. Dreischuh, G. G. Paulus, M. G. Schätzel, H. Walther, D. Neshev, W. Królikowski, and Yu. Kivshar, "Spatial phase dislocations in femtosecond laser pulses," J. Opt. Soc. Am. B **23**, 26–35 (2006).
[19] K. Yamane, Y. Toda, and R. Morita, "Ultrashort optical-vortex pulse generation in few-cycle regime," Opt. Express **20**, 18986–18993 (2012).
[20] M. Bock, J. Brunne, A. Treffer, S. König, U. Wallrabe, and R. Grunwald, "Sub-3-cycle vortex pulses of tunable topological charge," Opt. Lett. **38**, 3642–3645 (2013).
[21] S. Topuzoski and Lj. Janicijevic, "Fraunhofer diffraction of a LaguerreGaussian laser beam by fork-shaped grating," J. Modern Optics **58**, 138–145 (2011).
[22] S. Topuzoski and Lj. Janicijevic, "Conversion of high order Laguerre-Gaussian beams into Bessel beams of increased, reduced or zero-th order by use of a helical axicon," Optics Commun. **282**, 3426–3432 (2009).

[23] A. Mair, A. Vaziri, G. Weihs, and A. Zeilinger, "Entaglement of the orbital angular momentum states of photons," Nature **412**, 313–316 (2001).

[24] M. S. Soskin, V. N. Gorshkov, M. V. Vasnetsov, J. T. Malos, and N. R. Heckenberg, "Topological charge and angular momentum of light beams carrying optical vortices," Phys. Rev. A **56**, 4064–4075 (1997).

[25] M. S. Soskin and M. V. Vasnetsov, "Nonlinear singular optics," Pure Appl.Opt. **7**, 301–311 (1998).

[26] I. D. Maleev, A. M. Deykoon, G. A. Swartzlander, Jr., M. S. Soskin, and A. V. Sergienko, "Violation of conservation of topological charge in optical downconversion," in *Quantum Electronics and Laser Science Conference*, OSA Technical Digest, p. 99 (Optical Society of America, Washington, D.C., 1999).

[27] P. Hansinger, G. Maleshkov, I. L. Garanovich, D. V. Skryabin, D. N. Neshev, A. Dreischuh, and G. G. Paulus, "Vortex algebra by multiply cascaded four-wave mixing of femtosecond optical beams," Optics Express **22**, 11079–11089 (2014).

[28] H. Yu, H. Zhang, Y. Wang, S. Han, H. Yang, X. Xu, Z. Wang, V. Petrov, and J. Wang, "Optical orbital angular momentum conservation during the transfer process from plasmonic vortex lens to light," Nature Sci. Rep. **3** 3191 (2013).

[29] Lj. Janicijevic and S. Topuzoski, "Fresnel and Fraunhofer diffraction of a Gaussian laser beam by fork-shaped gratings," J. Opt. Soc. Am. A **25**, 2659–2669 (2008).

[30] I. V. Basistiy, V. Yu. Bazhenov, M. S. Soskin, and M. V. Vasnetsov, "Optics of light beams with screw dislocations," Opt. Commun. **103**, 422–428 (1993).

[31] W. M. Lee , X.-C. Yuan, and K. Dholakia, "Experimental observation of optical vortex evolution in a Gaussian beam with an embedded fractional phase step," Opt. Commun. **239**, 129–135 (2004).

[32] J. Romero, J. Leach, B. Jack, M. R. Dennis, S. Franke-Arnold, S. M. Barnett, and M. J. Padgett, "Entangled topological features of light," arXiv: 1101.3564v1.

[33] D. Cojoc, V. Garbin, E. Ferrari, L. Businaro, F. Romanato, and E. Di Fabrizio, "Laser trapping and micromanipulation using optical vortices," Microelectron. Eng. **78-79**, 125–131 (2005).

[34] K. Ladavac and D. G. Grier, "Microoptomechanical pumps assembled and driven by holographic optical vortex arrays," Optics Express **12**, 1144–1149 (2004).